

## BNL (Informal) Report

GALLEX Internal Report GX 78

November, 1995

RECEIVED

JAN 03 1995

DETERMINATION OF THE  $^{51}\text{Cr}$  SOURCE STRENGTH AT BNL\*

OS 11

J. Boger, R. L. Hahn, and Y. Y. Chu

Chemistry Department

Brookhaven National Laboratory

**Abstract**

Neutron activation analysis (NAA) and  $\gamma$ -ray counting have been used to measure the activity of 24 samples removed from the GALLEX radioactive Cr neutrino source. In 9.86% of the disintegrations,  $^{51}\text{Cr}$  decays with the emission of a 320-keV  $\gamma$ -ray. Counting this  $\gamma$ -ray provides a direct means to obtain the disintegration rates of the Cr samples. Based upon these disintegration rates, we obtain a strength of  $63.1 \pm 1.0$  PBq for the entire Cr source. The Cr source activity has also been obtained through measuring the  $^{51}\text{V}$  content of each sample by means of NAA.  $^{51}\text{V}$  is the decay daughter for all decay modes of  $^{51}\text{Cr}$ . Through neutron bombardment, radioactive  $^{52}\text{V}$  is produced, which decays with the emission of a 1434-keV  $\gamma$ -ray. By counting this  $\gamma$ -ray from NAA, we obtain a disintegration rate of  $62.1 \pm 1.0$  PBq for the entire source. These values are consistent with all other measurements of the source strength done at other GALLEX Laboratories.

\* Research carried out at Brookhaven National Laboratory under contract DEAC02-76CH00016 with the Office of High Energy and Nuclear Physics, U. S. Department of Energy.

MASTER

DISTRIBUTION OF THIS DOCUMENT IS UNLIMITED 35

## I. Introduction.

The well-known techniques of neutron activation analysis (NAA) and  $\gamma$ -ray counting have been used to measure the activity of 24 representative samples removed from the GALLEX 35.53-kg radioactive Cr neutrino source (Ref. 1). Each sample of approximately 0.5 to 1.0 g of solid material was dissolved in 10 ml of 6 M  $\text{H}_2\text{SO}_4$  at the Forschungszentrum Karlsruhe (FzK) and diluted to 100 ml; 80-ml portions were then shipped to Brookhaven National Laboratory (BNL) for subsequent analysis in order to determine the disintegration rate of the entire Cr source at end of bombardment, i.e., 6 A.M. June 20, 1994 at the Siloe' reactor in France.

$^{51}\text{Cr}$  has a half-life of 27.706 days (Ref. 2) and decays via electron capture to  $^{51}\text{V}$ . For 90.14% of the disintegrations,  $^{51}\text{Cr}$  decays directly to the ground state of  $^{51}\text{V}$ ; for the remaining 9.86 ( $\pm 0.05$ ) %,  $^{51}\text{Cr}$  decays to an excited state of  $^{51}\text{V}$ , followed by the emission of a 320-keV  $\gamma$ -ray to the ground state. Counting the number of emitted 320-keV  $\gamma$ -rays provides a direct means to obtain the disintegration rate of  $^{51}\text{Cr}$  in each sample. Results from this analysis are detailed in Section III.

The  $^{51}\text{Cr}$  disintegration rate of each sample has also been obtained by measuring the amount of the decay daughter,  $^{51}\text{V}$ , by way of NAA. To do this, we irradiated each Cr sample with a thermal neutron flux of  $\sim 10^{13} \text{ cm}^{-2} \text{ s}^{-1}$  in order to induce the  $^{51}\text{V}(n,\gamma)^{52}\text{V}$  reaction.  $^{52}\text{V}$  has a 3.746-min. half-life (Ref. 1) and emits a 1434-keV  $\gamma$ -ray with a branching ratio of 100%. By counting these 1434-keV  $\gamma$ -rays to determine the amount of  $^{51}\text{V}$  present in each sample, the disintegration rate of the Cr neutrino source has been derived. This method is discussed in Sections II and IV.

Because NAA derives the source strength in terms of the stable  $^{51}\text{V}$  nucleus, this method differs from the others that have been used to obtain the source strength, viz. calorimetry (Ref. 3), neutronics (Ref. 4),  $\gamma$ -scanning (Ref. 5), and  $\gamma$ -ray spectroscopy of the 320-keV  $\gamma$ -ray from the decay of  $^{51}\text{Cr}$  (Refs. 6, 7, and this paper.)

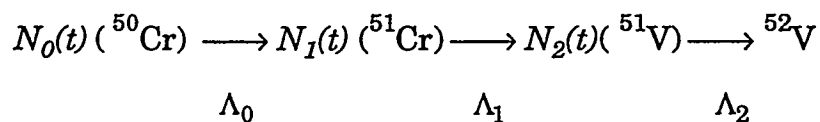
## II. Production of $^{51}\text{V}$ from $^{51}\text{Cr}$ Decay.

Stable  $^{51}\text{V}$  is the sole decay daughter of  $^{51}\text{Cr}$ . In principle, measuring the number of atoms of  $^{51}\text{V}$  that have grown into the Cr source after an interval of several  $^{51}\text{Cr}$  half-lives then determines the number of  $^{51}\text{Cr}$  atoms that were present at the end of the reactor bombardment (EOB).

However, this situation is complicated by the fact that  $^{51}\text{V}$  is not only produced from  $^{51}\text{Cr}$  decay after EOB, but also from its decay during the lengthy (24 days) Siloe' irradiation. One could simplify matters by chemically removing this  $^{51}\text{V}$  shortly after EOB to define a zero-time for the ingrowth of  $^{51}\text{V}$  from  $^{51}\text{Cr}$  decay. But such procedures would be difficult, requiring special equipment in hot cells to handle the intensely radioactive  $^{51}\text{Cr}$  source.

In this section, we investigate the relationships between the production of  $^{51}\text{Cr}$  and  $^{51}\text{V}$ , and show that it is not necessary to remove the  $^{51}\text{V}$  formed in the reactor to get an accurate value of the  $^{51}\text{Cr}$  content at EOB.

The processes that we consider during the irradiation of  $^{51}\text{Cr}$  are



where  $N_0(t)$ ,  $N_1(t)$ , and  $N_2(t)$  are the respective numbers of atoms, at instant  $t$  during the irradiation, of  $^{50}\text{Cr}$ ,  $^{51}\text{Cr}$ , and  $^{51}\text{V}$ . The respective reaction rates considered here, where  $\phi$  is the Siloe' flux and  $\sigma_i$  is the  $(n,\gamma)$  cross section for the specific nuclide, are

$$\Lambda_0 = \phi \sigma_0 = \text{Thermal-neutron capture rate on } ^{50}\text{Cr},$$

$$\Lambda_1 = \ln 2 / T_{1/2}(^{51}\text{Cr}) = \text{Decay rate of } ^{51}\text{Cr},$$

$$\Lambda_2 = \phi \sigma_2 = \text{Thermal-neutron capture rate on } ^{51}\text{V}.$$

[Note that the value of  $\Lambda_1$  barely changes if the  $^{51}\text{Cr}(n,\gamma)^{52}\text{Cr}$  burnup reaction is included as an additional disappearance mode for  $^{51}\text{Cr}$ , because the experimental upper limit (Ref. 8) for this cross section is small,  $< 10^{-23} \text{ cm}^2$ .]

The differential equations governing these reactions are

$$dN_i / dt = \Lambda_{i-1} N_{i-1}(t) - \Lambda_i N_i(t) \quad (\text{Eq. 1})$$

Their solutions are well known (Ref. 9):

$$N_0(t) = N_0(0) e^{-\Lambda_0 t}$$

$$N_1(t) = \frac{\Lambda_0 N_0}{(\Lambda_1 - \Lambda_0)} [e^{-\Lambda_0 t} - e^{-\Lambda_1 t}] \quad (\text{Eq. 2})$$

$$N_2(t) = \Lambda_1 \Lambda_0 N_0(0) \left\{ \left[ \frac{e^{-\Lambda_0 t}}{(\Lambda_1 - \Lambda_0)(\Lambda_2 - \Lambda_0)} \right] + \left[ \frac{e^{-\Lambda_1 t}}{(\Lambda_0 - \Lambda_1)(\Lambda_2 - \Lambda_1)} \right] \right\} \\ + \left[ \frac{e^{-\Lambda_2 t}}{(\Lambda_1 - \Lambda_2)(\Lambda_0 - \Lambda_2)} \right]$$

Of special concern here are (a) the value in Siloe' at EOB ( $t = T$ ) of the ratio of  $^{51}\text{V}$  to  $^{51}\text{Cr}$ ,  $N_2(T)/N_1(T)$ , and (b) the sensitivity of this ratio to changes in the neutron flux during the irradiation. We investigated these questions numerically by adopting the following representative values of the parameters:

$$\text{Target} = 40 \text{ kg of } 38\% \text{ } ^{50}\text{Cr}, \text{ and } N_0(0) = 1.786 \times 10^{26} \text{ atoms};$$

$$\text{Length of irradiation, } T = 24 \text{ days};$$

$$\sigma_0 = 15.9 \times 10^{-24} \text{ cm}^2;$$

$$\sigma_2 = 4.88 \times 10^{-24} \text{ cm}^2;$$

$$T_{1/2}(^{51}\text{Cr}) = 27.70 \text{ days, and } \Lambda_1 = 2.896 \times 10^{-7} \text{ s}^{-1}.$$

Calculations were done with Eq. 2 for a wide range of neutron fluxes, for 3, 6, 12 and  $30 \times 10^{13} \text{ cm}^{-2} \text{ s}^{-1}$ . [Note that, in the actual Siloe' irradiation, the values were  $\phi = 5.2 \times 10^{13} \text{ cm}^{-2} \text{ s}^{-1}$  (the average perturbed flux) and  $\sigma_0 = 17.2 \times 10^{-24} \text{ cm}^2$  (the effective cross section, including the contribution of the epithermal neutrons), well within the range of the parameters above; thus,  $\Lambda_0 = 8.94 \times 10^{-10} \text{ s}^{-1}$  and  $\Lambda_2 = 2.54 \times 10^{-10} \text{ s}^{-1}$ .]

The calculated results are very interesting. Although the values of  $N_1(T)$  and  $N_2(T)$  change with flux, the ratio,  $N_2(T)/N_1(T) = 0.33$ , remains constant to better than 1% over the factor of 10 change in flux.

We can understand why this ratio is constant if we solve the above differential equations, making the approximations that  $\Lambda_0$  and  $\Lambda_2 \ll \Lambda_1$ . The solutions are:

$$\begin{aligned}
 N_1(T) &= \frac{\Lambda_0 N_0(0)}{\Lambda_1} (1 - e^{-\Lambda_1 T}) \\
 N_2(T) &= \frac{\Lambda_0 N_0(0)}{\Lambda_1} (\Lambda_1 T - 1 + e^{-\Lambda_1 T}) \\
 \frac{N_2(T)}{N_1(T)} &= \frac{\Lambda_1 T}{(1 - e^{-\Lambda_1 T})} - 1.
 \end{aligned} \tag{Eq. 3}$$

We see that the ratio is independent of the neutron flux, depending only on  $\Lambda_1$  and  $T$ . For the values adopted here, this ratio =  $1.33 - 1 = 0.33$ , the result obtained above for the full equations.

Now, if a sufficiently long time,  $\Delta t = \tau > 10 T_{1/2}({}^{51}\text{Cr})$ , has passed after EOB, so that essentially all of the  ${}^{51}\text{Cr}$  has decayed to  ${}^{51}\text{V}$ , the ratio

$$\frac{N_2(\tau)}{N_1(T)} = \frac{N_1(T) + N_2(T)}{N_1(T)} = \frac{\Lambda_1 T}{(1 - e^{-\Lambda_1 T})} \tag{Eq. 4}$$

has the value 1.33. This definite factor, which is independent of the neutron flux and its variations, connects the total amount of  ${}^{51}\text{V}$  produced in the source both during and after the Siloe' irradiation to the amount of  ${}^{51}\text{Cr}$  present at EOB.

Thus, the amount of  ${}^{51}\text{Cr}$  in the source at EOB can be determined by measuring the  ${}^{51}\text{V}$  content of the source after most of the  ${}^{51}\text{Cr}$  has decayed, without any prior chemical separation of V from Cr. Inserting the actual parameters of the Siloe' irradiation in this relationship gives the value of the  ${}^{51}\text{Cr}$  source strength at EOB,  $D_1(T)$ , expressed as Bq of  ${}^{51}\text{Cr}$ ,

$$D_1(T) = \Lambda_1 N_1(T) = \frac{\Lambda_1 N_2(\tau)}{1.327} \tag{Eq. 5}$$

equal to  $2.5793 \times 10^9 \times (N_2 \text{ in units of } \mu\text{g } ^{51}\text{V})$  for the conditions of our measurements, where  $\tau > 340$  days. Expressed as Bq of  $^{51}\text{Cr}$  per g of Cr, the  $^{51}\text{Cr}$  source strength at EOB equals  $2.5793 \times 10^9 \times (N_2 \text{ in units of ppm } ^{51}\text{V})$ .

The above discussion assumes that there is no vanadium impurity in the enriched Cr target, so that the quantity  $N_2(t)$  of  $^{51}\text{V}$  in Eqs. 2-5 is due only to its formation from  $^{51}\text{Cr}$ . If, however, there were some vanadium impurity,  $N_2(0)$ , then an additional term would have to be inserted in Eq. 2 to include the burnup of this material in the irradiation,

$$N_2'(t) = N_2'(0)e^{-\Lambda_2 t}$$

Under the conditions of the irradiation,  $N_2'(T) = 0.9994 N_2'(0)$ ; the burnup is negligible. In Section IV below, we discuss the NAA measurement of  $N_2'(0)$ .

### III. Counting the 320-keV $\gamma$ -ray from $^{51}\text{Cr}$ .

#### A. Experimental techniques.

The sample number and concentration of each Cr sample received from FzK are listed in Table 1 in the first two columns. A Princeton Gamma-Tech Model LGC10ED intrinsic Ge detector was used to count the 320-keV  $\gamma$ -ray from the decay of  $^{51}\text{Cr}$ . To determine the disintegration rate of each sample, an absolute calibration of the detector's efficiency was made with a  $^{133}\text{Ba}$  radioactive point-source standard ( $3.513 \times 10^5 \text{ Bq} \pm 0.68\%$ ) produced and calibrated by the U.S. National Institute of Standards (NIST).

Radioactive  $^{133}\text{Ba}$  decays via electron capture with the emission of nine  $\gamma$ -rays with energies given here in keV (intensities in parentheses): 53.155 (2.17%), 79.621 (2.66%), 80.997 (33.5%), 160.605 (0.62%), 223.25 (0.46%), 276.397 (7.09%), 302.851 (18.40%), 356.005 (62.1%), and 383.851 (8.91%). The four highest energies bracket the 320-keV  $\gamma$ -ray produced in the decay of  $^{51}\text{Cr}$  and provide a convenient means to calibrate the detector.

The highest energy  $\gamma$ -ray produced in the decay of  $^{133}\text{Ba}$  is 383.851 keV. This fact indicates that the 437-keV line observed in our calibration spectrum was the result of random summing of two or more of the nine  $\gamma$ -rays listed above. This effect complicates the determination of the detector efficiency, as the intensities of the affected  $\gamma$ -rays are depleted from what would be observed were this summing not to occur.

We therefore need to know the contribution of each  $\gamma$ -ray to the 437-keV signal in order to correct for this effect. There are six combinations of  $\gamma$ -rays that produce the 437-keV signal ( $\gamma$ -rays that sum to other energies are negligibly small):

$$\begin{aligned}
 (1) & 356 + 81 \\
 (2) & 384 + 53 \\
 (3) & 276 + 161 \\
 (4) & 303 + 81 + 53 \\
 (5) & 223 + 161 + 53 \\
 (6) & 223 + 81 + 80 + 53
 \end{aligned}
 \tag{Eq. 6}$$

The amount that each  $\gamma$ -ray contributes to the 437-keV signal may be reasonably estimated from

$$\frac{e_i I_i}{\sum_i e_i I_i} \quad (\text{Eq. 7})$$

where  $e_i$  is the detector's efficiency for the  $i$ th  $\gamma$ -ray and  $I_i$  is the  $\gamma$ -ray intensity. The index  $i$  is over the first three summations listed in Eq. 6, as summations (4), (5), and (6) are small. Furthermore, because Eq. 7 is a ratio, the efficiencies  $e_i$  need not be absolute, and have been taken from an already existing efficiency curve for the Ge detector used in this measurement. The main contributions to the 437-keV peak are listed in Table 2, where we note that 96.3% of the 437-keV signal is due to the first sum in Eq. 6.

The calibration was done by counting the  $^{133}\text{Ba}$  source in the same geometry used to count the 320-keV  $\gamma$ -rays from the decay of  $^{51}\text{Cr}$ , i.e. approximately 10 cm in front of the detector. A pulser with a fixed-frequency output generated a signal in the  $\gamma$ -ray spectrum that was used as a deadtime correction to the number of counts. A  $\gamma$ -ray spectrum was obtained during 1.0 hr of counting. After subtraction for background, a net activity was obtained for each  $\gamma$ -ray, as well as for the 437-keV peak.

These activities provided the information to calculate counting efficiencies for the four  $\gamma$ -rays that bracketed the 320-keV  $\gamma$ -ray. The efficiencies of these  $\gamma$ -rays were plotted versus their energies, and a least-squares fit (linear over this energy interval on a log-log scale) was made in order to interpolate a value of 0.002355 as the efficiency of the 320-keV  $\gamma$ -ray.

Samples of the 24 Cr solutions provided by FzK were prepared for  $\gamma$ -ray counting in the following manner: An aliquot of 25  $\mu\text{l}$  was pipetted from each solution onto a piece of SPEX X-ray cell film of 0.25-mil thickness mounted on an aluminum counting card. The card and sample were then placed under a heat lamp in order to form a residue containing the

radioactive Cr. This residue was then covered by a second piece of film such that the sample was very nearly a point source encased in X-ray cell film. Tests showed that the film was not chemically attacked by the acidic residue. The  $^{51}\text{Cr}$  samples were then placed in front of the detector and counted in most cases for 2 hr, and for a few cases as much as 16 hrs. The first sample was counted 322 days after end of bombardment in the Siloe' reactor, and the last, 382 days (i.e., approximately 13 half-lives after EOB).

### B. Data analysis and uncertainties.

Fig. 1 shows the  $\gamma$ -ray spectrum for Sample 1.2, chosen as representative. Both the 320-keV  $\gamma$ -ray from the decay of  $^{51}\text{Cr}$  and the peak produced by the pulser are indicated in the figure. Deadtimes were typically less than 0.1%. The background rate adjacent to the 320-keV  $\gamma$ -ray peak was constant and allowed for a simple subtraction of an average background rate from the 320-keV photopeak. After correction for deadtime and background, the absolute disintegration rate of each sample was obtained from the net activity of the 320-keV  $\gamma$ -ray and extrapolated back to end of bombardment using the half-life of  $^{51}\text{Cr}$ . These disintegration rates per gram of Cr,  $(D/M)_i$ , are listed in the third column of Table 1.

Uncertainties in these disintegration rates are  $\sim 2\%$ . The statistical uncertainty was approximately 0.25% for each sample, although this value varied slightly depending on the total number of counts in the 320-keV photopeak and the background. Systematic uncertainties arose from the uncertainty in the mass of Cr pipetted ( $\sim 0.73\%$ ) and the uncertainty on the detector's efficiency ( $\sim 1.8\%$ ). This latter uncertainty was derived in part from information about the standard source provided by NIST. For example, the uncertainty on the activity of the  $^{133}\text{Ba}$  source is 0.68%, and

the average uncertainty in the branching ratios of the four  $\gamma$ -rays used in the calibration is  $\sim 1.3\%$ . Additional uncertainties include those on interpolating the detector efficiency for the 320-keV  $\gamma$ -ray,  $\sim 1\%$ , and on the 320-keV branching ratio,  $0.05\%$ .

### C. Strength of the $^{51}\text{Cr}$ neutrino source.

The arithmetic average of the disintegration rate per gram Cr, at end of bombardment for the 24 Cr samples,  $\sum_i (D/M)_i/24$ , was calculated to be  $1.782 \times 10^{12}$  Bq/g ( $\pm 7.5\% = 1\sigma$ ), with an error on the mean of  $1.52\%$ . Note that this standard deviation is significantly larger than the  $\sim 2\%$  error on an individual measurement. This indicates that the range of sample disintegration rates is greater than the error due to the method of measurement. This conclusion is supported by a Monte Carlo simulation of the sampling procedure, which produced a similar dispersion of several percent (Ref. 10).

We also obtain a mean disintegration rate per gram of Cr,

$$\frac{\sum_i [(D/M)_i M_i]}{\sum_i M_i} \quad (\text{Eq. 8})$$

at end of bombardment for all 24 solutions received from FzK, equal to  $1.777 \times 10^{12}$  Bq/g. We take the error on this mean to be  $1.52\%$ , as above, reflecting the fact that the estimated errors of the individual measurements done at BNL are small compared to the spread in the distribution of the values. (As expected, propagating the estimated errors on our individual measured values in Eq. 8 gives a much smaller error on the mean,  $\pm 0.4\%$ , that does not reflect the uncertainties caused by sampling.) From this mean value, a source strength of  $63.1 \pm 1.0$  PBq is derived for the entire 35.53 kg of Cr.

## IV. Neutron activation analysis.

### A. Experimental techniques.

Each of the samples listed in Table 1 was irradiated at least once in the BNL Medical Research Reactor (a total of 31 irradiations). This reactor was operated at 3 MW power, providing thermal neutrons at a flux of  $\sim 10^{13} \text{ cm}^{-2} \text{ s}^{-1}$ . These irradiations were done on four separate days over the course of a month: June 23, June 26, July 7, and July 21, 1995. As these  $\text{H}_2\text{SO}_4$  solutions were to be encapsulated in 1-ml capacity polypropylene holders for the irradiations, empty holders and holders containing  $\text{H}_2\text{SO}_4$  were first irradiated in order to see what backgrounds they produced in the  $\gamma$ -ray spectrum. Gamma-rays (energies in keV) for  $^{56}\text{Mn}$  (847, 1811, 2113),  $^{41}\text{Ar}$  (1294),  $^{24}\text{Na}$  (1369, 2754),  $^{38}\text{Cl}$  (1642, 2168), and  $^{37}\text{S}$  (3103), and their respective escape peaks, were identified. However, no  $\gamma$ -ray was observed in these test irradiations to have an energy that interfered with the 1434-keV  $\gamma$ -ray emitted in the decay of  $^{52}\text{V}$ .

Comparators containing a known amount of natural vanadium were simultaneously irradiated with the unknown Cr solutions. Irradiating and counting a vanadium comparator under the same conditions as the Cr unknown sample simplifies the neutron activation analysis. This relative method eliminates the need to know the values of (a) the  $^{51}\text{V}$  neutron capture cross section (which is the same for both sample and comparator), (b) the neutron flux during the irradiation, and (c) the detector counting efficiency (so long as the geometry used in counting the 1434-keV  $\gamma$ -ray is constant). Simply stated, this means

$$\frac{A_0(\text{sample})}{A_0(\text{comparator})} = \frac{\text{mass } ^{51}\text{V in Cr}}{0.9975 (\text{mass of comparator})} \quad (\text{Eq. 9})$$

where 0.9975 is the isotopic abundance of  $^{51}\text{V}$  in natural vanadium.

The chromium samples were prepared for neutron irradiation by pipetting 1.0-ml samples of the Cr solutions into individual polypropylene capped vials. The comparator samples, which contained 10  $\mu\text{g}$  of natural vanadium, were obtained by pipetting 1.0 ml of a 10- $\mu\text{g}/\text{ml}$  vanadium stock solution (in 0.6 M  $\text{H}_2\text{SO}_4$ ) into other polypropylene vials.

These vials were then placed under a heat lamp to reduce the volume of solution in each vial by approximately one half, to insure against excessive expansion of the liquid samples during irradiation. Vials containing one chromium sample and one vanadium comparator were then placed together in the same plastic rabbit in the pneumatic-tube facility at the reactor for a simultaneous irradiation period of 2 (sometimes 4) minutes. Simultaneous irradiation of the sample and comparator minimizes any differences in neutron flux in the two samples that may occur during the irradiation.

After irradiation, the activated samples were placed in capped glass vials for double containment and quickly transferred to a counting room with a low background to count the 1434-keV  $\gamma$ -ray from the decay of  $^{52}\text{V}$ . The Gamma-Tech intrinsic Ge detector is the same one described in Sec. IIIA. The glass vial was placed in a lead housing with a collimating hole pointing towards the detector. A lead absorber, 6880- $\text{mg}/\text{cm}^2$  thick, was placed between the sample and the detector to reduce the intensity of the  $^{51}\text{Cr}$  320-keV  $\gamma$ -ray, which was a major source of random summing. Counting generally began 6 to 8 minutes after end of irradiation. Typically, the Cr sample was first counted for two minutes, then alternated with the

comparator. The overall counting period for both the sample and comparator generally ended 35 to 40 minutes after the end of the irradiation (8 to 10 half-lives).

A fixed-frequency pulser was used to generate a known number of pulses in the  $\gamma$ -ray spectrum for a deadtime correction to the number of observed events. Fig. 2(a) shows the NAA  $\gamma$ -ray spectrum for Cr sample 1.2. Compared to the  $^{51}\text{Cr}$  spectrum shown in Fig. 1 for the same sample, Fig. 2 contains additional lines that are due to the neutron activation of the sample, the sample holder, and the sulfuric acid. Fig. 2(b) shows the  $\gamma$ -ray spectrum for the vanadium comparator used in the same irradiation. Both the 1434-keV  $\gamma$ -ray from the decay of  $^{52}\text{V}$  and the peak produced by the pulser are indicated in the figure. Other  $\gamma$ -rays are mainly due to  $^{38}\text{Cl}$  and  $^{37}\text{S}$ .

Two NAA irradiations were also done to measure the amount of vanadium impurity in samples of the solid enriched Cr metal that had not been exposed to the Siloe' neutron flux. The irradiation and counting details of these experiments were analogous to those used for the liquid samples described above.

### **B. Data analysis.**

After correcting the activities for deadtimes and backgrounds, a least-squares computer code, CLSQ (Ref. 11), specifically written for the analysis of radioactive decay data, was used to obtain sample and comparator  $^{52}\text{V}$  activities at the same time, the end of irradiation. These activities were obtained in most cases by fitting the decay curve with a single component, the half-life of  $^{52}\text{V}$ , 3.746 min. An example of one of these fits is shown by the line in Fig. 3. In a few cases where high

background rates were apparent, the best fits were obtained with the inclusion of a second decaying component, the impurity  $^{38}\text{Cl}$ , with a half-life of 37.2 min.

The activities for the sample and comparator were then inserted in Eq. 9 to obtain the mass of  $^{51}\text{V}$  in each Cr sample; see the fourth column of Table 1. The corresponding concentration of  $^{51}\text{V}$  in ppm ( $10^{-6} \text{ g } ^{51}\text{V} / \text{g Cr}$ ) is given in the fifth column. From Section II above, the factor  $2.5793 \times 10^9$  converts ppm of  $^{51}\text{V}$  to the disintegration rate of  $^{51}\text{Cr}$  in Bq/g at end of bombardment at the Siloe' reactor. These values are listed in the sixth column of Table 1.

Results from 3 of the 31 irradiations were rejected during the data analysis. These are indicated by the letter "R" in parentheses in Table 1. The first irradiation of sample 2.2 was rejected due to leakage of the sample holder. The other two irradiations were eliminated based on a statistical analysis of the  $^{52}\text{V}$  activities produced in the vanadium comparators at the end of irradiation. The irradiation conditions were found to be quite stable from run to run and day to day. This is indicated by an average comparator activity of  $1.734 \times 10^5$  ( $\pm 2.3\% = 1\sigma$ ) counts per minute for the entire 10  $\mu\text{g}$  of vanadium. Comparator activities for Sample 2.9 and the second value for Sample 2.4 were outside two standard deviations of the average comparator activity and were rejected.

### C. Strength of the Cr source.

For the remaining 28 values, the arithmetic average of the ppm  $^{51}\text{V}$  was calculated as  $\sum_i (\text{ppm } ^{51}\text{V})_i / 28 = 679.3$  ( $\pm 8.76\%$ ) ppm, with the error on the mean being  $\pm 1.66\%$ . This  $1\sigma$ -error is similar to that for the analogous measurements from counting the 320-keV  $\gamma$ -ray ( $\pm 7.5\%$ ) and again

represents the spread in sample activities, not the error on an individual measurement. This average value translates into a disintegration rate of  $1.752 \times 10^{12}$  Bq/g of Cr at end of bombardment.

However, several samples were irradiated twice (see Table 1) and thus provide a means to estimate the precision of an individual measurement. To estimate this uncertainty, we calculated the average of these duplicate measurements and its standard deviation, found to be 2.7% of the average value. Thus, a conservative estimate of the reproducibility of an individual NAA measurement, including the systematic errors, is 4-5%.

A mean value of the ppm  $^{51}\text{V}$  may also be calculated via the following prescription,  $\sum_i (\mu\text{g } ^{51}\text{V})_i / \sum_i (\text{g Cr})_i$ , analogous to the case of the 320-keV  $\gamma$ -ray (see Eq. 8). The mean value obtained is 677.8 ppm  $^{51}\text{V}$ , a small change from the arithmetic average of 679.2 derived above. This is equivalent to a mean disintegration rate of  $1.748 \times 10^{12}$  Bq/g at EOB.

As we had done with the results of Eq. 8, we take the realistic error on this mean value to be that of the arithmetic average,  $\pm 1.66\%$ , again reflecting the fact that the estimated errors of the individual measurements done at BNL are small compared to the spread in the distribution of the values. (As expected, propagating the estimated errors on our individual measured values gives a smaller error on the mean,  $\pm 0.97\%$ , that does not reflect the uncertainties caused by sampling.) From this mean value, a source strength of  $62.1 \pm 1.0$  PBq is derived for the entire 35.53 kg of Cr.

The results from the NAA measurements of the solid enriched Cr metal showed that the vanadium impurity levels,  $N_2(0)$ , were very low, as might be expected since the chromium had initially been transformed to a gaseous compound so it could be mass separated by gas centrifugation. An upper limit derived from two samples was  $\leq 5$  ppm of vanadium, i.e., <

0.8% of the vanadium concentrations found in the chromium samples that had been irradiated in Siloe'. As such, no correction for this impurity was applied to the NAA results discussed above.

## V. Conclusions.

For the full Cr source, we have obtained a mean value of  $63.1 \pm 1.0$  PBq at EOB from counting the 320-keV  $\gamma$ -ray produced in the radioactive decay of  $^{51}\text{Cr}$ . From NAA analysis of the  $^{51}\text{V}$  decay daughter, we have derived a value of  $62.1 \pm 1.0$  PBq. These two values are consistent within their experimental uncertainties.

The Cr source strength has also been evaluated at other GALLEX Laboratories and by other methods. These methods break down into four categories:

- 1) calorimetry (Ref. 3).
- 2) reactor monitoring (Refs. 4, 5).
- 3) ionization chamber assay (Ref. 6).
- 4) gamma-ray spectroscopy (Ref. 7 and this work).

The first two methods are integral, i.e. they measure the disintegration rate of the entire 35.53 kg of Cr. The third and fourth methods, like those discussed here, depend on sampling. Table 3 lists the methods used, the institutions where the measurements were made, and the quoted strengths of the source, as well as the results from the work reported here. We note from Table 3 that all values for the source strength, irrespective of the method employed to obtain its strength, are in agreement within their respective errors.

Observe from Table 3 that the three institutions that measured the 320-keV  $\gamma$ -ray from the decay of  $^{51}\text{Cr}$  obtained very similar results. However, differences existed between the methods used. For example, the Max-Planck Institute (MPI)-Heidelberg used a  $^{51}\text{Cr}$  standard source in solution to calibrate the efficiency of its detector (Ref. 12), whereas FzK used a standardized solution containing 10 radionuclides but not  $^{51}\text{Cr}$  (Ref. 13). The advantage of using  $^{51}\text{Cr}$  as a standard is that it eliminates any systematic error introduced in the analysis by the branching ratio for the 320-keV  $\gamma$ -ray, a feature exploited only by MPI, but one whose effect had little consequence on the final results. Furthermore, as standards in solutions were used by both MPI and FzK to calibrate their detectors, they also performed their  $\gamma$ -ray spectroscopy on liquid samples. BNL, as discussed above, used a solid calibration source and solid samples that approximated point sources. The similarity of the results, however, suggests that these differences of geometry and calibration used by the three laboratories are not significant.

## **VI. Acknowledgments.**

We thank the staff of the BNL Medical Research Reactor for their help and cooperation in doing the NAA irradiations. We express our appreciation to members of the BNL Medical Department for providing health physics support and for the use of their counting room. Special thanks go to Dr. R. von Ammon of FzK for arranging the four shipments of the radioactive solutions to BNL.

Table 1. Results of BNL measurements on the 24 Cr samples.

Cr No.	Samples Conc. <i>M</i> (g/100ml)	320 keV $\gamma$		Neutron Activation	
		<i>D/M</i> (EOB) ( $10^{12}$ Bq/g)	$^{51}\text{V}$ ( $\mu\text{g}$ )	$^{51}\text{V}$ (ppm)	<i>D/M</i> (EOB) ( $10^{12}$ Bq/g)
1.2	0.7055	1.922	4.971	704.6	1.817
			4.959	702.9	1.813
1.3	0.7086	1.615	4.320	609.6	1.572
1.4	0.9395	1.914	6.859	730.1	1.883
			6.802	724.0	1.867
1.5	0.7574	1.765	5.001	660.2	1.703
1.8	0.9689	1.726	6.319	652.2	1.682
1.9	0.8100	1.797	5.486	677.3	1.747
2.2	0.4338	1.946	3.000	689.8	(R) 1.779
			3.532	814.2	2.100
2.3	0.4327	2.023	3.226	745.6	1.923
2.4	0.4708	1.829	3.236	687.4	1.773
			3.599	764.5	(R) 1.972
2.6	0.7322	1.641	4.553	621.8	1.604
2.7	0.6740	1.798	4.770	707.7	1.825
2.9	0.6617	1.719	4.788	723.6	(R) 1.866
3.2	0.3590	1.669	2.168	603.8	1.557
			2.489	693.3	1.788
3.3	0.6680	1.605	3.851	576.5	1.487
			4.149	621.0	1.602
3.4	0.6768	1.715	4.468	660.1	1.703

3.5	0.6499	1.712	4.281	658.7	1.699
3.6	0.7626	1.761	5.114	670.6	1.730
3.8	0.7440	1.754	4.905	659.2	1.700
3.9B	0.7041	1.903	5.304	753.3	1.943
4.3	0.6546	2.137	5.470	835.6	2.155
4.4	0.6087	1.717	3.839	630.6	1.627
			4.099	673.3	1.737
4.7	0.9825	1.708	6.407	652.1	1.682
4.8	0.8325	1.760	5.584	670.7	1.730
4.9B	0.7065	1.639	4.410	624.2	1.610

---

Table 2. Major contributions to the 437-keV sum peak.

$E_\gamma$ (keV)	% of 437-keV sum peak
276	1.25
356	96.3
384	2.47

Table 3. Measured  $^{51}\text{Cr}$  strengths (PBq at EOB).

Method	GALLEX group	Result
Calorimetry	Grenoble/ Saclay	$61.9 \pm 3.0$
Neutronics	Grenoble/ Saclay	$64.4 \pm 5.2$
Gamma Scanning	Grenoble/ Saclay	$64.0 \pm 5.0$
Ionization chamber	Saclay	$61.3 \pm 0.8$
Ge(HP) $\gamma$ -spectra	Karlsruhe	$63.1 \pm 0.9$
Ge(HP) $\gamma$ -spectra	Heidelberg	$63.2 \pm 0.9$
Ge(HP) $\gamma$ -spectra	Brookhaven	$63.1 \pm 1.0$
Vanadium yield	Brookhaven	$62.1 \pm 1.0$

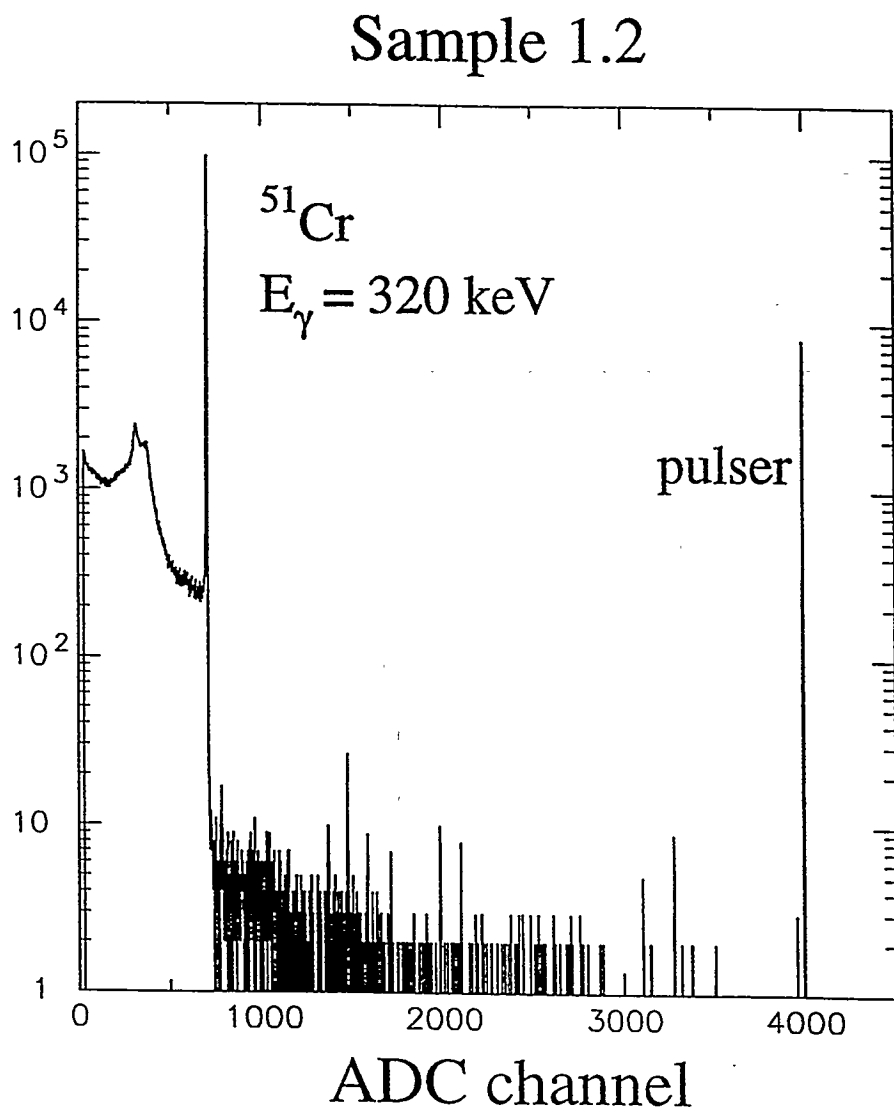


Fig. 1. Gamma-ray spectrum for sample 1.2 in  $\text{H}_2\text{SO}_4$ . The 320-keV  $\gamma$ -ray of  $^{51}\text{Cr}$  and the pulser line are indicated.

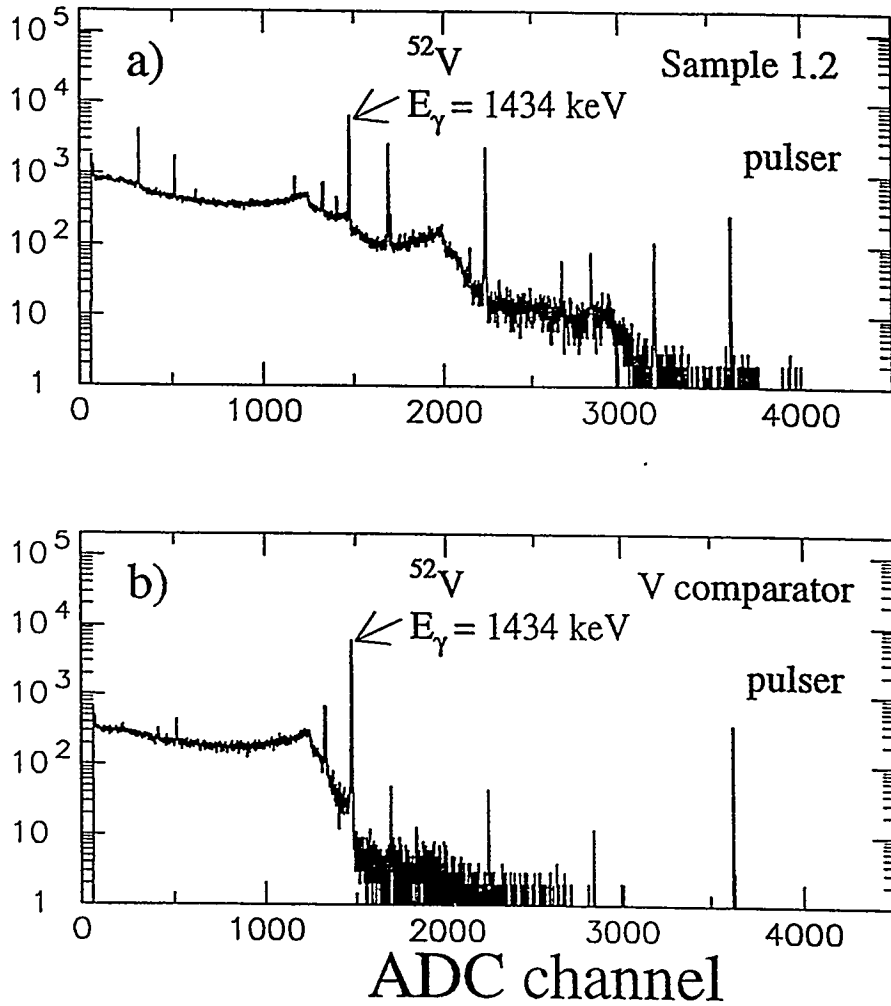


Fig. 2. (a) Gamma-ray spectrum from NAA at BNL for sample 1.2 in  $\text{H}_2\text{SO}_4$ . The 1434-keV  $\gamma$ -ray of  $^{52}\text{V}$  and the pulser line are indicated. (b) Same, but for vanadium comparator.

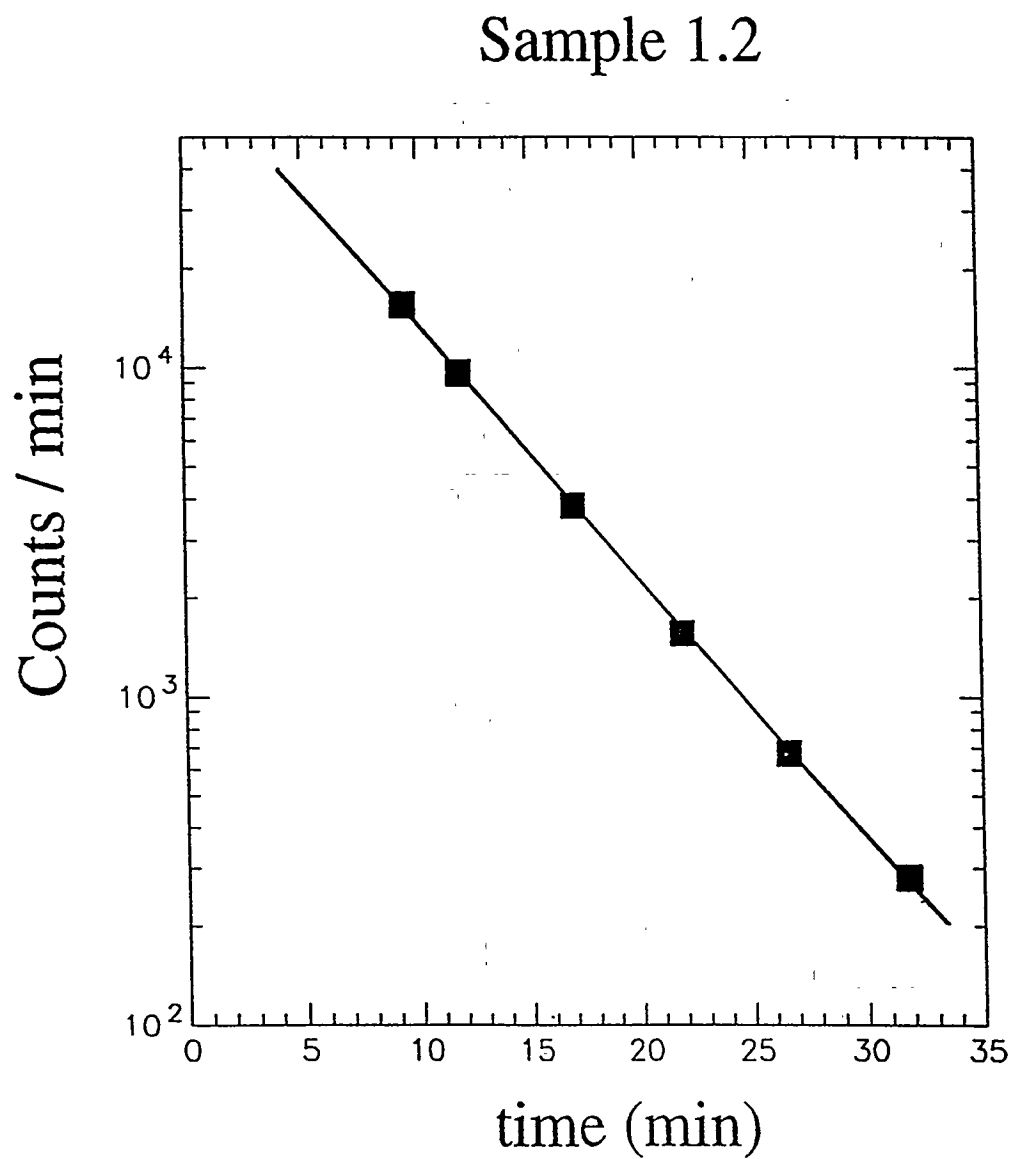


Fig.3. Decay curve of  $^{52}\text{V}$  for sample 1.2 from NAA at BNL. The solid squares are the measured count rates corrected for dead time, and the line is a least-squares fit (CLSQ, Ref. 11) to the data.

## References.

1. GALLEX collaboration: P. Anselmann et al., *Phys. Lett.* **B342**, 440 (1995).
2. U. Schoetzig and H. Schrader, PTB-Bericht **PTB-Ra-16/4** (Braunschweig, 1993).
3. Saclay Group, *GALLEX Note GX-58* (Oct. 1994).
4. A. Bevilacqua, *GALLEX Note GX-59* (Sept. 1994).
5. E. Bellotti et al., *GALLEX Note GX-63* (Nov. 1994).
6. M. Cribier, *GALLEX Note GX-64* (Nov. 1994).
7. GALLEX collaboration, *GALLEX Note GX-79* (July 1995).
8. S. Katcoff, private communication.
9. G. Friedlander, J. W. Kennedy, E. S. Macias and J. M. Miller, *Nuclear and Radiochemistry*, 3rd ed., (Wiley, New York, 1981).
10. J. Rich, *GALLEX Note GX-68* (March 1995).
11. J.B. Cumming, "CLSQ: The Brookhaven decay curve analysis program," from *Applications of Computers to Nuclear and Radiochemistry*, ed. by G. D. O'Kelly, U.S. Atomic Energy Commission Report, **NAS-NS 3107**, pp.25-33 (1963).
12. W. Hampel, private communication.
13. R. von Ammon, private communication.

## DISCLAIMER

This report was prepared as an account of work sponsored by an agency of the United States Government. Neither the United States Government nor any agency thereof, nor any of their employees, makes any warranty, express or implied, or assumes any legal liability or responsibility for the accuracy, completeness, or usefulness of any information, apparatus, product, or process disclosed, or represents that its use would not infringe privately owned rights. Reference herein to any specific commercial product, process, or service by trade name, trademark, manufacturer, or otherwise does not necessarily constitute or imply its endorsement, recommendation, or favoring by the United States Government or any agency thereof. The views and opinions of authors expressed herein do not necessarily state or reflect those of the United States Government or any agency thereof.

The first part of the document discusses the importance of maintaining accurate records of all transactions. It emphasizes that every entry should be supported by a valid receipt or invoice. This ensures transparency and allows for easy verification of the data.

In the second section, the author outlines the various methods used to collect and analyze the data. This includes both primary and secondary data collection techniques. The primary data was gathered through direct observation and interviews, while secondary data was obtained from existing reports and databases.

The third section details the statistical analysis performed on the collected data. It describes the use of descriptive statistics to summarize the data and inferential statistics to test hypotheses. The results of these analyses are presented in a clear and concise manner, highlighting the key findings of the study.

Finally, the document concludes with a discussion of the implications of the findings. It suggests that the results have significant implications for the field and offers recommendations for further research. The author also acknowledges the limitations of the study and expresses gratitude to those who assisted in the research process.